Nanoscale

Volume 1 | Number 1 | Jan 2013 | Pages 1–100

Nanoscale

www.rsc.org/nanoscale

ROYAL SOCIETY OF CHEMISTRY

ROYAL SOCIETY OF CHEMISTRY

www.rsc.org/nanoscale

Journal Name

COMMUNICATION

Ni^{3+} doped monolayer layered double hydroxide nanosheets as efficient electrodes for supercapacitors

Yufei Zhao,[a] Qing Wang,[ab] Tong Bian,[a] Huijun Yu,[a,b] Hua Fan,[ab] Chao Zhou,[a] Li-Zhu Wu,[a] Chen-Ho Tung,[a] Dermot O'Hare[c] and Tierui Zhang*[a]

Ni^{3+} **doped NiTi layered double hydroxide (NiTi-LDH) monolayer nanosheets with particle size ~20 nm and a thickness of ~0.9 nm have been successfully prepared through a facile bottom-up approach. These NiTi-LDH monolayer nanosheets exhibit excellent supercapacitor performances, including high specific pseudocapacitance (2310 F g^{-1} at 1.5 A g^{-1}) and long durability compared with bulk LDH, owning to highly exposed conductive Ni^{3+} spieces (NiOOH) which lead to the increasing mobility rate of surface charge and electrolyte-transfer. Therefore, this work is expected to take a significant step towards exploring novel 2D monolayer electrode materials with unique physical and chemical properties for applications in energy storage and conversion.**

With the seriously increased power and energy demands from portable electronics to various microdevices, supercapacitors, very promising next-generation energy storage devices, have received tremendous attention in recent years, mainly due to their fast charge and discharge rate, high power density, and long durability.[1,2] So far, pseudocapacitive carbon based nanomaterials (carbon nanotubes, graphene oxides, polymer and other carbon composites) combined with transition metal (Ru, Ni, Co, Mn, etc.) hydroxides/oxides have been extensively exploited for supercapacitors.[3] Despite of the great progress made recently, the following issues still need to be addressed. The inherently poor conductivity of pseudocapacitive electrodes limits the migration of electrons, leading to relatively poor energy output. Moreover, the extremely serious aggregation of electroactive sites tends to reduce the accessible surface area for participating electrolyte, and thus results in a decrease of capacitance behavior.[4] Therefore, it is urgent to develop novel electrodes by rational design and synthesis on the side of structure and composition.

Recently, the synthesis of ultrathin 2D monolayer materials have experienced an epoch paradigm shift since the isolation of graphene. These all-surface-atom materials exhibit exceptional physical and chemical characters, and have been widely applied in photoelectrocatalysis, bioimaging, optoelectronic devices, and so on.[5] Theoretical and experimental studies in the Xie group demonstrated that abundant atomic defects in monolayer semiconductors can notably increase the mobility rate of surface electron and then enhance catalytic performances significantly. This major breakthrough in handling physical and chemical characters of materials provide a new method for solving key problems of energy storage and conversion.[6] Motivated by this breakthrough, we take the challenge of developing ultrathin monolayer capacitor-active materials with atomic thickness to improve the electron-transfer efficiency and thus electrochemical capacitance performances.

Monometallic nickel or cobalt hydroxides are widely used for electrochemical capacitors due to their specific 2D layered structure with higher specific capacitance.[7] However, they normally exhibit low durability owing to severe polymorphic transformation during charging process, which limits their further industrial applications.[8] Many researchers tried to develop bimetallic analogues which may exhibit stable structural characteristics.[9] Among them, layered double hydroxides (LDHs), a family of important layered clays, are promising electroactive materials for supercapacitors owing to their ideal redox behavior, low cost, environmental friendliness and comprehensive utilization of homogeneously dispersed transition metal sites.[10] Recently, Wei's group demonstrated that electrochemical capacitors, core-shell NiAl-LDH and NiAl-LDH@polymer *in situ* grown on nickel foam, displayed high specific capacitances of ~800 F g^{-1} and ~700 F g^{-1}, respectively.[11] Besides, a hybrid NiAl-LDH/graphene electrode possesses a maximum specific capacitance of ~800 F g^{-1}.[12] The electrochemical behaviors of these materials are still not satisfied enough to meet the requirements for the high performance of next-generation energy storage devices. This probably due mainly to their relatively large diameter of 0.2 - 5 μm and thickness of 6 - 40 nm containing more than 10 LDH monolayers, resulting in fewer exposed surface atoms. The surface atoms of LDHs involving in faradaic redox reactions play a key role in controlling the efficiency of active metal sites and electron-transfer rate.[13]

Herein, we designed and prepared one novel type of sophisticated monolayer NiTi-LDH (monolayer-NiTi-LDH) nanosheets with almost fully exposed pseudocapacitance active (001) facets and then proved its excellent electrochemical capacitive performance. In view of its fantastic monolayer structure, monolayer-NiTi-LDH exhibits sufficiently improved electrocapacitance (2310 F g^{-1} at 1.5 A g^{-1}, based on pristine active LDH), which is unprecedented and 6 times higher than that of the bulk conterpart. Futhermore, it can maintain remarkable rate capability and long durability. The monolayer-NiTi-LDH nanosheets with highly exposed chemically reactive sites and a large specific surface area ensure efficient supercapacitive reaction. The Ni^{3+} defects in monolayer-NiTi-LDH promote the electron accumulation as well as transportation, and simultaneously buffer the large volume change of active sites in recycling process. This facile strategy for the preparation of monolayer LDH nanosheets with a large number of exposed surface active defects is very efficient and highly expected to be a general one to improve supercapacitive behavior remarkably for practical energy storage devices, etc.

The monolayer-NiTi-LDH nanosheets were prepared by an *in-situ* growth process in the reverse microemulsion formed by surfactant, co-surfactant and water. The general synthesis protocol is illustrated in Scheme 1. It is worth noting that in pure water system, the layer stacking of the LDH layer is hard to be controlled, and only LDH multilayer structures can be produced (Scheme S1).
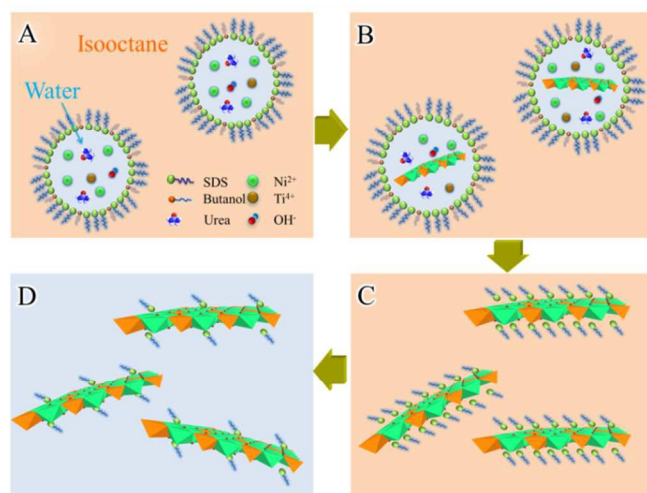
Scheme 1 Schematic representation for the formation of monolayer-NiTi-LDH nanosheets in micelle: (A) metal salts and urea mix in water droplets; (B) LDH starts to form during the hydrolysis of urea; (C) the monolayer-NiTi-LDH nanosheets form in isooctane; (D) monolayer-NiTi-LDH nanosheets are transferred into water surrounding after cleaning.

Transmitted electron microscopy (TEM) image (Fig. 1A) reveals that monolayer-NiTi-LDH exhibits a plate-like shape with particle size around ~20 nm and the hexagonal lattice with a = 0.30 nm corresponding to the exposed (001) facets of the monolayer-NiTi-LDH phase was observed in the HRTEM image (Fig. 1B).[14] The thickness of the monolayer-NiTi-LDH nanosheets was determined by atomic force microscopy (AFM) to be an amazing ~0.9 ± 0.1 nm (Fig. 1C, 1D). While the bulk NiTi-LDH (bulk-NiTi-LDH) sample

prepared by the conventional coprecipitation route displays rather larger particle size (~100 nm) and thickness (~12 nm) (Fig. S1A, S1B). And the comparative bulk NiAl-LDH sample (bulk-NiAl-LDH) exhibits a particle size of ~100 nm and a thickness of ~6 nm (Fig. S1C, S1D). The thickness of the monolayer-NiTi-LDH nanosheets is nearly the same as that of previously reported monolayer MgAl-LDH,[15] which was demonstrated as the sum of crystallographic thickness (0.48 nm) of the LDH monolayer and an adsorbed surfactant monolayer (~0.5 nm). If LDH nanoparticles consist of more than two single layers, the thickness values of nanoparticles would be certainly no less than 1 nm with the intercalation of interlayer anions. Such a thickness of ~0.9 nm unambiguously confirms the formation of monolayer-NiTi-LDH nanosheets.[16] While bulk-NiTi-LDH and bulk-NiAl-LDH exhibit a larger packing of ~17 and ~8 layers, respectively, based on the interlayer spacing of 0.72 nm and 0.76 nm obtained from XRD data and previous reports (Fig. S2).[17] The smallest particle size and monolayer morphology of monolayer-NiTi-LDH guarantee a sufficient exposure of chemically reactive sites, thus facilitating the increment of specific pseudocapacitance activity.
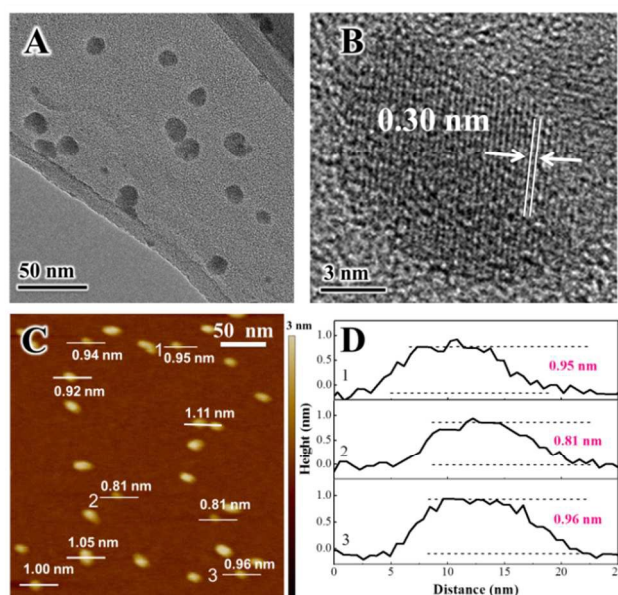
Fig. 1 Characterizations for the monolayer-NiTi-LDH nanosheets. A) TEM image; B) HRTEM image; C) AFM image and D) the corresponding height profiles; the numbers from 1 to 3 in (D) correspond to the numbers from 1 to 3 in (C).

X-ray diffraction (XRD) patterns of the as-synthesized bulk-NiTi-LDH and bulk-NiAl-LDH are shown in Fig. S2a and S2b, the intense (003) Bragg reflections clearly indicate the well crystalline structure, which is in accordance with the above TEM observations. However, XRD date of monolayer-NiTi-LDH nanosheets in Fig. S2c only exhibits three very weak diffraction peaks at around 25°, 35° and 61°, respectively. The strong characteristic basal plane diffraction peaks of LDHs are not observed, suggesting that the host sheets are not thick enough to give Bragg reflection along the c-axis. This further proves the highly delaminated nature of monolayer-NiTi-LDH formed in the reverse microemulsion system. Besides, the presence of adsorbed species in monolayer-NiTi-LDH was further

evidenced using Fourier transform infrared spectroscopy (FT-IR) (Fig. S3). The intense IR transmittance bands centered at 2198 cm^{-1} and 1384 cm^{-1} can be ascribed to the stretching vibration of CNO$^-$ and CO$_3^{2-}$, from the incomplete decomposition of urea, showing the existence of both CNO$^-$ and CO$_3^{2-}$ in monolayer-NiTi-LDH. Additionally, the peaks at 2958, 2918, 2850 cm^{-1} are related to the stretching vibrations of CH$_2$ and CH$_3$, implying the adsorption of organic molecules on the surface of the monolayer-NiTi-LDH nanosheets.[17a]

Cyclic voltammograms (CVs) of Ni-containing LDH electrodes at a scan rate of 5 mV s^{-1} were employed to evaluate the pseudocapacitive activity. As shown in Fig. 2A, the CV curves show two typical peaks, corresponding to the typical capacitive behavior of Ni^{2+}/Ni^{3+} with an assistance of OH$^-$. Compared with bulk-NiTi-LDH, monolayer-NiTi-LDH possesses much larger area of CV curves, exhibiting that the layer stacking and the particle size of LDHs play key roles in electrochemical performance. The galvanostatic charge-discharge curves of these LDHs at 1.5 A g^{-1} also exhibited a typical pseudocapacitive behavior (Fig. 2B). The specific capacitance of monolayer-NiTi-LDH calculated from the discharge curve is as high as 2310 F g^{-1} (based on the active LDH) at 1.5 A g^{-1}, which is 6 times higher than that of bulk-NiTi-LDH (393 F g^{-1}) and 29 times higher than that of the well-studied bulk-NiAl-LDH (77 F g^{-1}), further demonstrating the excellent capacitance of single-layer LDH electrode. The specific capacitance for monolayer-NiTi-LDH is considered quite high for metal hydroxides/oxides-based conventional electrode materials without any carbon or metal foam supports in large-power supercapacitors.[11a, 13a, 18] The rate capability is another key factor for the practical application of supercapacitors. The specific capacitances of those three LDHs materials derived from the discharging curves as a function of current densities from 1.5 to 30 A g^{-1} are shown in Fig. S4 and Fig. 2C. Noticeably, all electrodes exhibit a well-defined discharge plateau, showing that they are highly active under the current densities studied. At 30 A g^{-1}, the specific capacitance retains 53% (decreasing from 2310 to 1206 F g^{-1}) for monolayer-NiTi-LDH, whereas bulk-NiTi-LDH drops from 393 to 20 F g^{-1}, and bulk-NiAl-LDH almost loses the specific capacitance completely. This demonstrates that the capacitive performance of monolayer-NiTi-LDH is much superior to the other two Ni-containing LDHs. The excellent specific capacitance and high-rate capability of monolayer-NiTi-LDH are mainly attributed to its exceptional monolayer structure with highly exposed chemically reactive sites. This monolayer nanostructure provides more accessible active sites of anions and sufficient diffusion paths for the electrolyte ions (K$^+$ and OH$^-$) as well as the increased electrical conductivity, which will be further discussed in the next section.

Besides the specific capacitance, the electrode's stability in alkaline solution is also a key factor for commercialized pseudocapacitors and batteries. The long-term charge-discharge cycling stability for monolayer-NiTi-LDH was investigated at 12 A g^{-1} in the potential window of 0 to 0.45 V (Fig. S5). After 3000 cycles, the capacitance of bulk-NiTi-LDH drops from 393 to 130 F g^{-1} with ~67% off, and bulk-NiAl-LDH electrode loses ~76.0% of its original capacitance. In the case of monolayer-NiTi-LDH,

however, the capacitance remains at 1895 F g^{-1} with ~82.0% retention.
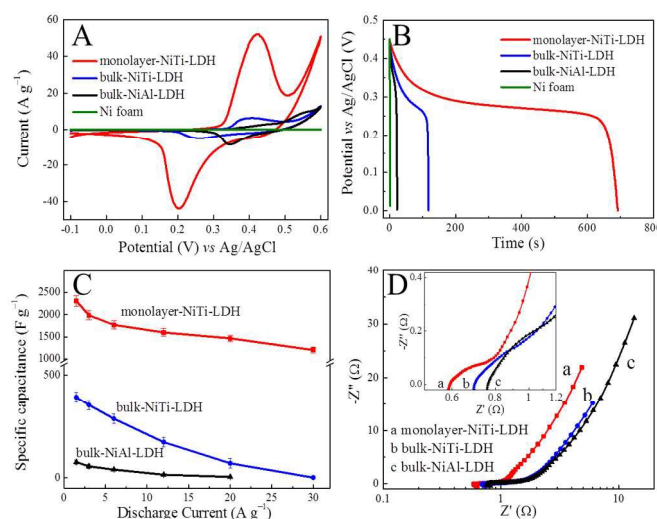

Fig. 2 (A) CV curves; (B) galvanostatic discharge curves; (C) current density dependent on the specific capacitance; and (D) Nyquist plots of EIS for monolayer-NiTi-LDH, bulk-NiTi-LDH and bulk-NiAl-LDH.

The ultrahigh specific capacitance and good durability make the monolayer-NiTi-LDH electrode very promising for pseudocapacitance devices. The better cycling stability of monolayer LDH compared with bulk LDH electrode further testifies the advantage of monolayer structure for energy storage. This enhanced electrochemical behavior was further confirmed by the much lower interfacial charge-transfer resistance of monolayer-NiTi-LDH from electrochemical impedance spectroscopy (EIS) measurements. As shown in Fig. 2D, the equivalent series resistance for monolayer-NiTi-LDH was calculated to be 0.6 Ω, demonstrating that monolayer-NiTi-LDH exhibits the best electrical conductivity compared with bulk-NiTi-LDH and bulk-NiAl-LDH. The above results are in well agreement with the CV and galvanostatic behaviors of all those three LDH samples, clearly proving that the monolayer structured LDH has the lowest resistance and facilitates the efficiency of electron transfer. For Ni-containing LDH supercapacitors, the redox reaction includes the migration of electrons on the surface of LDH electrodes associated with the reversible reaction of OH$^-$ from electrolyte solution.[13b] The better conductivity of monolayer-NiTi-LDH implies a faster charge transfer from the chemically reactive sites to the charge collector. In comparison to bulk LDHs, the monolayer structure of monolayer-NiTi-LDH can promote the effective exposure of chemically reactive sites and the transfer rate of electrons.

In order to explore the excellent supercapacitive behavior of monolayer-NiTi-LDH, low temperature electron paramagnetic resonance (EPR) was investigated to shed light on the chemical surroundings of Ni ions in the monolayer-NiTi-LDH nanosheets (Fig. 3A and Fig. S6). Monolayer-NiTi-LDH exhibits a very broad signal with g = 2.128 (peak-to-peak line width (ΔH_{pp}) greater than 297 G at 110 K), 2.556 and 2.236, respectively, which is characteristic of Ni^{3+}.[19] The peaks with g = 1.996 and 2.030 can be assigned to Ti^{3+} and O$^-$ species, respectively, which are in

accordance with our previous report (Fig. S6B).[17a] However, no obvious signals are detected for bulk-NiTi-LDH and bulk-NiAl-LDH (Fig. S7).[20] Xie *et al.* reported that ultrathin exfoliated nanosheets containing oxygen defects shorten the ion diffusion pathway length and increase the utilization ratio of active sites, which may result in high specific electrochemical performance.[21] It is therefore proposed that the electrical active Ni^{3+} species in monolayer-NiTi-LDH play a key role in facilitating charge transfer and thus enhancing the supercapacitive behavior.
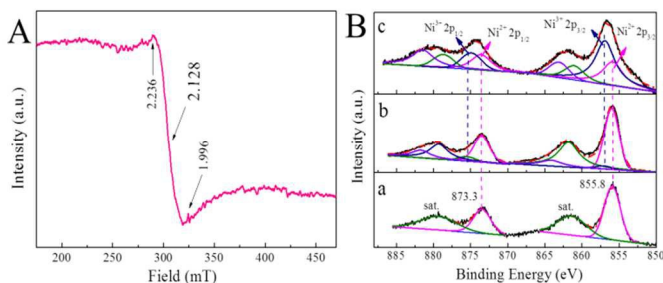

Fig. 3 (A) EPR spectrum of as-prepared monolayer-NiTi-LDH at 110 K under Ar atmosphere. (B) Ni 2p XPS spectra of (a) bulk-NiAl-LDH, (b) bulk-NiTi-LDH and (c) monolayer-NiTi-LDH.

X-ray photoelectron spectroscopy (XPS) was employed to detect the surface compositions and chemical states of all LDH samples. In Fig. 3Ba, the Ni 2p XPS spectrum of bulk-NiAl-LDH exhibits two typical Ni^{2+} $2p_{3/2}$ and Ni^{2+} $2p_{1/2}$ peaks centered at 855.8 eV and 873.3 eV, respectively.[22] With the replacement of Al^{3+} in the layer of bulk-NiAl-LDH by Ti^{4+}, that is bulk-NiTi-LDH, a new typical Ni^{3+} $2p_{3/2}$ peak appears (Fig. 3Bb).[23] Moreover, by decreasing the particle size of bulk-NiTi-LDH as well as the stacking number, the Ni^{3+} $2p_{3/2}$ defect peak of monolayer-NiTi-LDH increases significantly accompanied with a reduction of the Ni^{2+} $2p_{3/2}$ peak (Fig. 3Bc). The Ni^{3+} surface states in monolayer-NiTi-LDH account for ~66.0%, *versus* ~6.0% in bulk-NiTi-LDH. The growing amount of surface Ni^{3+} ions in monolayer-NiTi-LDH is mainly ascribed to the layer stacking effect. It is clear that the Ni^{3+} sites are obviously formed by more oxygen vacancy defects, and exist in the form of NiOOH, which imposes a significant effect on the electrical conductivity of materials and promotes the efficiency of charge transfer.[3a]

It has been proved that the chemically oxidized NiOOH is extremely active in electrochemical reaction, and its electrical conductivity is about 10^{-5} S cm^{-1}, which is apparently higher than that of $Ni(OH)_2$ (10^{-8} S cm^{-1}).[24] Besides, the proton diffusion coefficient decreases three orders of magnitude from 3.4 • 10^{-8} cm^2 s^{-1} for NiOOH to 6.4 • 10^{-11} cm^2 s^{-1} for $Ni(OH)_2$.[25] Therefore, the chemically oxidized NiOOH doped in Ni-containing LDHs contributes to the decreasing in the conductive resistance of materials, leading to the significantly improved supercapacitive performance. It is known that $Ni(OH)_2$ will be oxidized into NiOOH during the first charge cycle, and most of NiOOH cannot be reduced to Ni^{2+} state. Although some chemically reactive Ni^{2+} sites are reduced, the electrochemically oxidized Ni^{3+} states can apparently increase the conductivity of the layer structure.[18b] This similar phenomena has also been reported by Pralong *et al.* in Co-containing materials that the chemically oxidized CoOOH has a higher

conductivity compared with electrochemically oxidized CoOOH, because of more Co^{4+} states introduced during chemical oxidation process,[26] and the electrical conductivity of chemically oxidized CoOOH (10^{-2} S cm^{-1}) is actually much higher than that of electrochemically oxidized CoOOH (10^{-5} S cm^{-1}). Based on this point, it can be concluded that Ni^{3+} cations can be produced during the electrochemical oxidation process, and the Ni^{3+} state introduced would contribute greatly to a much lower EIS. Therefore, the improved rate performance of the monolayer-NiTi-LDH nanosheets is closely related to the generation of more Ni^{3+} cations.

The electronic structure of Ni^{3+} defects in Ni-containing LDHs was further studied by periodic density functional theory (DFT) calculations. Monolayer-NiTi-LDH with Ni^{3+} defect states was modeled by removing hydrogen atoms from the Ni nearest OH groups, thereby creating an H vacancy (V_H) and a Ni^{3+} defect (Fig. S8). As revealed in Fig. S9, for an ideal NiTi-LDH system, the valence band top is mainly consisted by O 2p and Ni 3d orbitals while the conduction band bottom is constructed by Ti 3d orbitals. This indicates that an ideal pristine NiTi-LDH exhibits a classic semiconductor property. However, the spin-up states of Ni^{3+} doped monolayer-NiTi-LDH are gapless and show remarkably improved density of states (DOS) values around the Fermi level (Fig. 4), demonstrating a half-metallic characteristic.[13b] As the efficiency of electron transport in solid phase has a great relationship with the DOS of the band edge, the considerably promoted DOS values arising from the existence of Ni^{3+} states confirm the improved carrier mobility and electrical conductivity of Ni^{3+} doped monolayer-NiTi-LDH, which are responsible for the enhanced electrochemical performance.
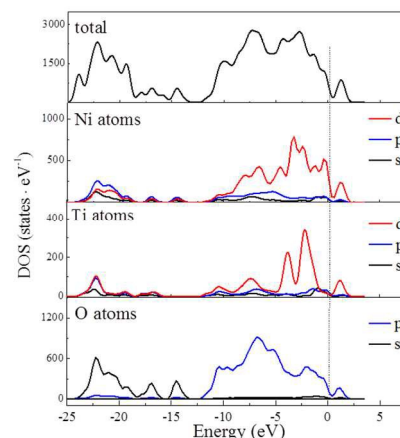

Fig. 4 Total DOS (TDOS) and Partial DOS (PDOS) of Ni^{3+} doped monolayer-NiTi-LDH.

Conclusions

In summary, Ni^{3+} doped NiTi-LDH monolayer nanosheets with excellent pseudocapacitive performance have been successfully synthesized through a facile bottom-up approach. The monolayer-NiTi-LDH nanosheets exhibit a maximum specific capacitance of 2310 F g^{-1}, strikingly higher than that of bulk-NiTi-LDH (377 F g^{-1}) and bulk-NiAl-LDH (77 F g^{-1}). In addition, monolayer-NiTi-LDH also shows excellent rate capability (82.0 % capacitance was remained at a large current density of 12 A g^{-1}) and good cycling performance. EIS spectra

demonstrate the remarkably improved pseudocapacitive performance of monolayer-NiTi-LDH is due to the promoted charge transfer compared with the bulk sample. The abundant Ni^{3+} surface active sites in monolayer-NiTi-LDH serve as more conductive species as evidenced by EPR, XPS and DFT calculations. Overall, this work is expected to take a significant step towards exploring novel advanced 2D monolayer electrode materials with unique physical and chemical properties for applications in energy storage and conversion devices.

Notes and references

ªKey Laboratory of Photochemical Conversion and Optoelectronic Materials, Technical Institute of Physics and Chemistry, Chinese Academy of Sciences, Beijing, 100190, P. R. China. Fax: +86 10 62554670; Tel: +86 10 82543428
E-mail: tierui@mail.ipc.ac.cn
bUniversity of Chinese Academy of Sciences, Beijing, 10049, P. R. China
cChemistry Research Laboratory, Department of Chemistry, University of Oxford, Mansfield Road, Oxford OX1 3TA, United Kingdom

† Electronic Supplementary Information (ESI) available: Experiment details and additional characterization data. See DOI: 10.1039/c000000x/

1. P. Simon and Y. Gogotsi, *Nat. Mater.*, 2008, **7**, 845.
2. X. X. Liu, C. Wang, Y. B. Dou, A. W. Zhou, T. Pan, J. B. Han and M. Wei, *J. Mater. Chem. A*, 2014, **2**, 1682.
3. (a) G. Wang, L. Zhang and J. Zhang, *Chem. Soc. Rev.*, 2012, **41**, 797; (b) C. Z. Yuan, H. B. Wu, Y. Xie and X. W. Lou, *Angew. Chem. Int. Ed.*, 2014, **53**, 1488; (c) P. Balaya, *Energy Environ. Sci.*, 2008, **1**, 645; (d) L. Y. Zhang, C. H. Tang and H. Gong, *Nanoscale*, 2014, **6**, 12981.
4. J. R. Miller and P. Simon, *Science*, 2008, **321**, 651.
5. (a) Y. F. Sun, Z. H. Sun, S. Gao, H. Cheng, Q. H. Liu, F. C. Lei, S. Q. Wei and Y. Xie, *Adv. Energy Mater.*, 2014, **4**, 10.1002/aenm.201300611; (b) Z. Sun, T. Liao, Y. Dou, S. M. Hwang, M. S. Park, L. Jiang, J. H. Kim and S. X. Dou, *Nat. Commun.*, 2014, **5**, 3813; (c) H. Li, J. Wu, Z. Yin and H. Zhang, *Acc. Chem. Res.*, 2014, **47**, 1067; (d) Y. Peng, L. Shang, T. Bian, Y. Zhao, C. Zhou, H. Yu, L.-Z. Wu, C.-H. Tung and T. Zhang, *Chem. Commun.*, 2015, DOI: 10.1039/C5CC00136F.
6. (a) C. Z. Wu, X. L. Lu, L. L. Peng, K. Xu, X. Peng, J. L. Huang, G. H. Yu and Y. Xie, *Nat. Commun.*, 2013, **4**, 2431; (b) S. Gao, Y. Sun, F. Lei, L. Liang, J. Liu, W. Bi, B. Pan and Y. Xie, *Angew. Chem. Int. Ed.*, 2014, **53**, 12789.
7. (a) J. Yan, Z. Fan, W. Sun, G. Ning, T. Wei, Q. Zhang, R. Zhang, L. Zhi and F. Wei, *Adv. Funct. Mater.*, 2012, **22**, 2632; (b) H. Chang, J. Kang, L. Chen, J. Wang, K. Ohmura, N. Chen, T. Fujita, H. Wu and M. Chen, *Nanoscale*, 2014, **6**, 5960.
8. X.-P. Gao and H.-X. Yang, *Energy Environ. Sci.*, 2010, **3**, 174.
9. (a) J. W. Zhao, J. L. Chen, S. M. Xu, M. F. Shao, D. P. Yan, M. Wei, D. G. Evans and X. Duan, *J. Mater. Chem. A*, 2013, **1**, 8836; (b) X. Liu, R. Ma, Y. Bando and T. Sasaki, *Adv. Mater.*, 2012, **24**, 2148.
10. (a) Q. Wang and D. O'Hare, *Chem. Rev.*, 2012, **112**, 4124; (b) R. Ma, X. Liu, J. Liang, Y. Bando and T. Sasaki, *Adv. Mater.*, 2014, **26**, 4173.
11. (a) M. Shao, F. Ning, Y. Zhao, J. Zhao, M. Wei, D. G. Evans and X. Duan, *Chem. Mater.*, 2012, **24**, 1192; (b) J. Han, Y. Dou, J. Zhao, M. Wei, D. G. Evans and X. Duan, *Small*, 2013, **9**, 98.
12. Z. Gao, J. Wang, Z. Li, W. Yang, B. Wang, M. Hou, Y. He, Q. Liu, T. Mann, P. Yang, M. Zhang and L. Liu, *Chem. Mater.*, 2011, **23**, 3509.
13. (a) P. Vialat, C. Mousty, C. Taviot-Gueho, G. Renaudin, H. Martinez, J. C. Dupin, E. Elkaim and F. Leroux, *Adv. Funct. Mater.*, 2014, **24**, 4831; (b) J. Zhao, J. Chen, S. Xu, M. Shao, Q. Zhang, F. Wei, J. Ma, M. Wei, D. G. Evans and X. Duan, *Adv. Funct. Mater.*, 2014, **24**, 2938; (c) H. Chen, L. Hu, M. Chen, Y. Yan and L. Wu, *Adv. Funct. Mater.*, 2014, **24**, 934.
14. Y. Zhao, M. Wei, J. Lu, Z. L. Wang and X. Duan, *ACS Nano*, 2009, **3**, 4009.
15. (a) J. Liang, R. Ma, N. Iyi, Y. Ebina, K. Takada and T. Sasaki, *Chem. Mater.*, 2010, **22**, 371; (b) A. I. Khan and D. O'Hare, *J. Mater. Chem.*, 2002, **12**, 3191.
16. Z. P. Liu, R. Z. Ma, M. Osada, N. Iyi, Y. Ebina, K. Takada and T. Sasaki, *J. Am. Chem. Soc.*, 2006, **128**, 4872.
17. (a) Y. Zhao, B. Li, Q. Wang, W. Gao, C. J. Wang, M. Wei, D. G. Evans, X. Duan and D. O'Hare, *Chem. Sci.*, 2014, **5**, 951; (b) Y. Zhao, P. Chen, B. Zhang, D. S. Su, S. Zhang, L. Tian, J. Lu, Z. Li, X. Cao, B. Wang, M. Wei, D. G. Evans and X. Duan, *Chem. Eur. J.*, 2012, **18**, 11949.
18. (a) J. T. Li, W. Zhao, F. Q. Huang, A. Manivannan and N. Q. Wu, *Nanoscale*, 2011, **3**, 5103; (b) X. Wang, C. Y. Yan, A. Sumboja, J. Yan and P. S. Lee, *Adv. Energy Mater.*, 2014, **4**, 10.1002/aenm.201301240; (c) H. B. Wu, H. Pang and X. W. Lou, *Energy Environ. Sci.*, 2013, **6**, 3619.
19. R. Stoyanova, E. Zhecheva, R. Alcantara and J. L. Tirado, *J. Phys. Chem. B*, 2004, **108**, 4053.
20. A. Davidson, J. F. Tempere, M. Che, H. Roulet and G. Dufour, *J. Phys. Chem.*, 1996, **100**, 4919.
21. J. F. Xie, X. Sun, N. Zhang, K. Xu, M. Zhou and Y. Xie, *Nano Energy*, 2013, **2**, 65.
22. M. Hu, X. R. Gao, L. X. Lei and Y. M. Sun, *J. Phys. Chem. C*, 2009, **113**, 7448.
23. A. F. Carley, S. D. Jackson, J. N. O'Shea and M. W. Roberts, *Surf. Sci.*, 1999, **440**, L868.
24. G. Barral, S. Maximovitch and F. NjanjoEyoke, *Electrochim. Acta*, 1996, **41**, 1305.
25. S. Motupally, C. C. Streinz and J. W. Weidner, *J. Electrochem. Soc.*, 1995, **142**, 1401.
26. (a) V. Pralong, A. Delahaye-Vidal, B. Beaudoin, B. Gerand and J. M. Tarascon, *J. Mater. Chem.*, 1999, **9**, 955; (b) V. Pralong, A. Delahaye-Vidal, B. Beaudoin, J. B. Leriche and J. M. Tarascon, *J. Electrochem. Soc.*, 2000, **147**, 1306.

Nanoscale Accepted Manuscript